

## The Contraction Coefficient of a Free-Surface Flow Under Gravity Entering a Region Beneath a Semi-Infinite Plane

L. H. Wiryanto<sup>1,\*</sup> and H. B. Supriyanto<sup>2</sup>

<sup>1</sup> Department of Mathematics, Bandung Institute of Technology, Jalan Ganesha 10 Bandung, Indonesia.

<sup>2</sup> Faculty of Art and Design, Bandung Institute of Technology, Jalan Ganesha 10 Bandung, Indonesia.

Received 24 September 2012; Accepted (in revised version) 14 November 2012

Available online 29 November 2012

---

**Abstract.** Borda's mouthpiece consists of a long straight tube projecting into a large vessel, where fluid enters the tube in a free surface flow that tends to become uniform far downstream in the tube. A two-dimensional approximation to this flow under gravity in the upper part of the tube leads to an evaluation of the contraction coefficient, the ratio of the constant depth of the uniform flow to the width of the tube. The analysis also applies to flow under gravity past a sluice gate, if the semi-infinite wall above the channel is rotated to the vertical. The contraction coefficient depends upon the Froude number  $F$ , and is generally less than the zero gravity value of  $1/2$  that is approached as  $F \rightarrow \infty$ .

**AMS subject classifications:** 65E05, 76B07, 76M15

**Key words:** Borda's mouthpiece, free-surface flow, boundary integral equation, contraction coefficient.

---

### 1. Introduction

Borda's mouthpiece consists of a long straight tube projecting into a large vessel, as illustrated in Fig. 1. The fluid in the vessel flows into the tube with a free surface detached from the wall of the tube, and eventually in a uniform stream far from its entry into the tube. When gravity is neglected, the flow in the tube is symmetric about the centre of the tube, and the ratio between the width of the uniform stream and the diameter of the tube (called the *contraction coefficient*) is known to be  $1/2$  [1]. The symmetric flow assumption in Borda's mouthpiece is not valid when gravity is included, but in this paper we ignore the flow into the lower part of the tube (indeed, the flow in the entire shaded part of

---

\*Corresponding author. Email address: leo@math.itb.ac.id (L. H. Wiryanto)

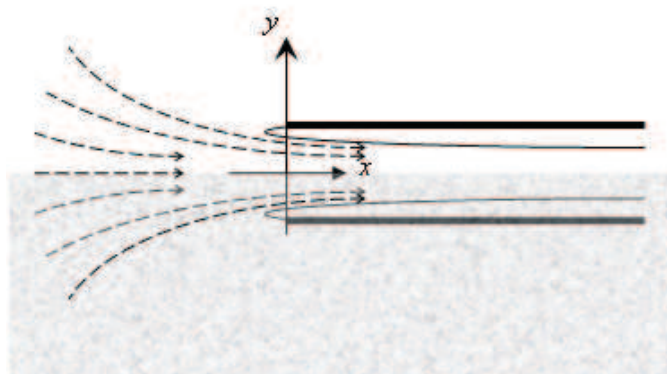


Figure 1: Borda's mouthpiece flow.

Fig. 1) and consider a two-dimensional approximation of the flow into its upper part. The contraction coefficient of the assumed two-dimensional flow under gravity is calculated in this paper.

Our analysis also applies to flow under gravity past a sluice gate, if the semi-infinite horizontal wall above the channel in the corresponding two-dimensional configuration shown in Fig. 2(a) is rotated to the vertical. A numerical solution has been found for the free surface flow under a sluice gate from deep water, and the modified flow due to the channel terminating in a waterfall was also considered [2, 3]. Most sluice gate flows discussed elsewhere are for fluid of finite depth upstream [4–6] — cf. also [7–9] more recently. The solutions are characterised by uniform and supercritical flow far downstream, and supercritical or subcritical flow far upstream. A wave train occurs when the upstream flow is subcritical. Binder and Vanden Broeck [10] considered possible multiple disturbances at the bottom of the channel or the free surface, such as due to a submerged obstacle or a pressure distribution or a sluice gate. They obtained solutions in which the radiation condition is satisfied — i.e. waves are formed near the gate and disappear, so the flow tends to be uniform far upstream. However, all solutions involve uniform and supercritical flow far downstream. We found this characteristic behaviour in our numerical solution for the flow from infinitely deep water [2] — but also a back flow near the edge of the gate and a stagnation point for small Froude number, and free surface separation from the vertical wall at an angle  $2\pi/3$  or  $-5\pi/6$  to the vertical axis [3]. This limiting case agrees with Vanden-Broeck & Tuck [11], who considered a free surface flow locally near a vertical wall — cf. also Dagan & Tulin [12] for analysis of the flow near a stagnation point. A solution with a stagnation point was also obtained for an inclined wall until the wall makes the angle  $\pi/3$  to the horizontal and the stream leaves the wall horizontally [14], when the free-surface flow leaves the boundary smoothly without any stagnation point. Mc Cue and Forbes [13] solved free-surface flows emerging from a semi-infinite plate with constant vorticity, a stagnation point occurs at the end of the plate and the free surface leaves the plate at detachment angle  $2\pi/3$  for small Froude number.

In this paper, we use a boundary element method to solve an integral equation involv-

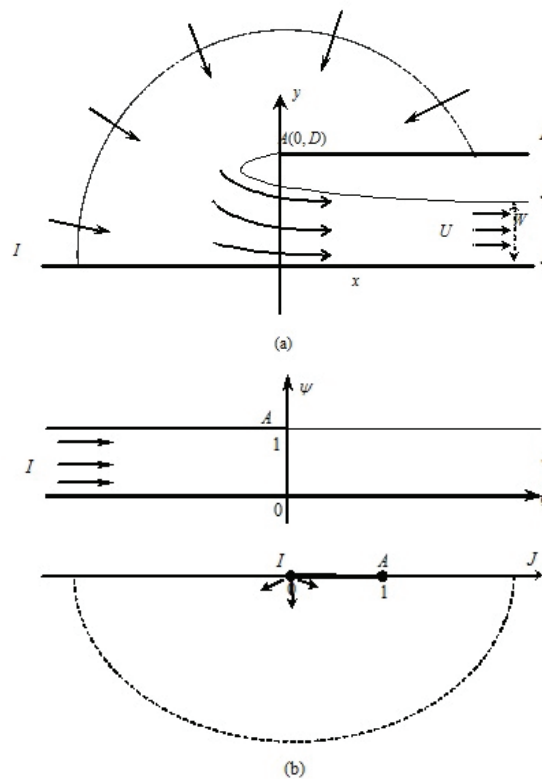


Figure 2: Sketch of the two-dimensional flow entering a slit (a) in physical  $z$ -plane, (b) in  $f$  and  $\zeta$ -planes.

ing a complex hodograph variable. This method has previously been used to solve some of the free surface flows mentioned above — e.g. see [15, 16] for a free surface flow producing one or two jets, or free surface flows caused by a line sink or source [17–19]. The resulting system of nonlinear algebraic equations can be solved by Newton iteration, so provided it converges the point coordinates of the free surface can be calculated for supercritical flow — i.e. for Froude number  $F = U/\sqrt{gW} > 1$ , where  $U$  is the velocity and  $W$  is the depth of the uniform flow in the tube far downstream ( $g$  is the gravitational acceleration). We obtain the relation between  $F$  and the contraction coefficient ratio  $W/D$ , where  $D$  is the width of the entrance (the slit) measured from the bottom of the channel, and find that  $W/D \rightarrow 1/2$  as  $F \rightarrow \infty$ .

## 2. Problem Formulation

We consider a steady two-dimensional irrotational flow of an inviscid incompressible fluid under gravity in a large vessel of semi-infinite depth, with a semi-infinite wall shown in the horizontal above the vessel bottom in Fig. 2(a). From far upstream (denoted by I), the fluid enters the slit of width  $D$  as a free surface flow under the wall and eventually becomes uniform with depth  $W$  and velocity  $U$  far downstream (denoted by J). The flow

is assumed to leave the edge of the wall tangentially. We choose Cartesian coordinates with the  $x$ -axis along the bottom, and the  $y$ -axis vertically upward and passing through the leading edge of the horizontal wall. The flow is described by the complex potential  $f(z) = \phi(x, y) + i\psi(x, y)$ , a function of the complex variable  $z = x + iy$ , such that the complex velocity is  $df/dz = u - iv$  where  $(u, v)$  is the velocity vector.

For convenience, we work in dimensionless variables using  $U$  as the characteristic velocity and  $W$  the characteristic length. Thus our task is to solve the boundary value problem

$$\phi_{xx} + \phi_{yy} = 0 \tag{2.1}$$

in the flow domain, subject to the dynamic condition represented by the Bernoulli equation expressed as

$$\frac{1}{2}F^2 (\phi_x^2 + \phi_y^2) + \eta = \frac{1}{2}F^2 + 1 \tag{2.2}$$

along the free surface  $y = \eta(x)$  given the continuity of pressure there, and the kinematic condition

$$\frac{\partial \phi}{\partial \bar{n}} = 0 \tag{2.3}$$

at both solid and free boundaries of the fluid (where  $\bar{n}$  is the local normal at the boundary). The Froude number is

$$F = \frac{U}{\sqrt{gW}},$$

under the non-dimensionalisation, with the left-hand side in Eq. (2.2) the downstream component and the constant right-hand side the contribution in the uniform flow upstream.

When the potential function  $\phi(x, y)$  and the free boundary  $y = \eta(x)$  satisfying Equations (2.1)–(2.3) are obtained, then  $\eta$  at the separation point  $A$  can be evaluated to render the contraction coefficient. However, on assuming  $\phi = 0$  and  $\psi = 0$  at the origin of the physical  $z$ -plane, the flow domain in the complex potential  $f$ -plane is a strip of width 1 from  $I$  to  $J$  as shown in Fig. 2(b) — and alternatively, we may proceed by introducing a hodograph variable  $\Omega = \tau - i\theta$  such that

$$\frac{df}{dz} = e^\Omega. \tag{2.4}$$

Thus instead of the potential function  $\phi(x, y)$  we seek the variable  $\Omega$  as a function of an artificial variable  $\zeta = \xi + i\rho$ , with the lower half plane in  $\zeta$  becoming the flow domain corresponding to the strip in the  $f$ -plane under the conformal mapping

$$f = i - \frac{1}{\pi} \log \zeta. \tag{2.5}$$

As also shown in Fig. 2(b), the flow upstream at  $I$  is mapped into  $\zeta = 0$  and the separation point  $A$  is mapped into  $\zeta = 1$ , such that the free surface corresponds to  $\xi > 1$  and  $\rho = 0$ .

In summary, instead of determining  $\phi(x, y)$  we solve for the hodograph variable  $\Omega$  as a function of  $\zeta$  satisfying the Laplace equation, where the dynamical condition (2.2) becomes

$$\frac{1}{2}F^2 e^{2\tau} + \eta = \frac{1}{2}F^2 + 1, \quad (2.6)$$

and the kinematic condition (2.3) is expressed in terms of the angle  $\theta$  of the streamline

$$\theta = \begin{cases} 0, & \xi < 0 \\ -\pi, & 0 < \xi < 1 \end{cases} \quad (2.7)$$

for the solid boundary but is unknown for the free boundary  $\xi > 1$ . We obtain  $\theta$  from Eq. (2.6), and  $\tau$  and  $\eta$  must be expressed as functions of  $\theta$ .

The relation between  $\theta$  and  $\tau$  is obtained as follows. We apply Cauchy's integral theorem for  $\Omega$  along the real  $\zeta$ -axis and the lower semi circle  $|\zeta| \rightarrow \infty$ . Thus for any  $1 < \xi < \infty$ ,

$$\Omega(\xi) = \frac{i}{\pi} \int_{-\infty}^{\infty} \frac{\Omega(s)}{s - \xi} ds, \quad (2.8)$$

and taking the real part of Eq. (2.8) yields

$$\tau(\xi) = \log \left| \frac{\xi}{1 - \xi} \right| + \frac{1}{\pi} \int_1^{\infty} \frac{\theta}{s - \xi} ds, \quad (2.9)$$

after substituting the value of  $\theta$  given by (2.7). Meanwhile,  $\eta(\xi)$  is obtained from Eqs. (2.4) and (2.5) such that

$$\frac{dz}{d\zeta} = -\frac{e^{\Omega}}{\pi\zeta}. \quad (2.10)$$

On integrating the imaginary part from  $\xi$  to  $\infty$ , since  $\eta = 1$  at infinity we obtain

$$\eta(\xi) = 1 + \frac{1}{\pi} \int_{\xi}^{\infty} \frac{e^{-\tau} \sin \theta}{s} ds. \quad (2.11)$$

The relations (2.9) and (2.11) substituted in (2.6) then produce the integral equation for  $\theta$ , to be solved in order to determine the free surface from Eq. (2.10). The value of  $x$  is obtained from the real part, and the ordinates are given by Eq. (2.11).

### 3. Zero Gravity Solution

Let us first determine the analytical solution in the absence of gravity for comparison. The flow contains a singularity at the separation point, where the stream leaves the solid boundary to form a free surface at  $\zeta = 1$ . The hodograph variable  $\Omega$  should be considered via analytic function

$$\chi(\zeta) = \frac{\Omega}{\sqrt{\zeta - 1}}. \quad (3.1)$$

The singular point  $\zeta = 1$  is the order of a square root [20]. We write Eq. (3.1) along the real axis on invoking Eq. (2.7) and zero gravity, when Eq. (2.6) gives  $\tau = 0$  for  $\xi > 1$  and we have

$$\chi(\xi) = \begin{cases} -i\tau/\sqrt{1-\xi}, & \xi < 0 \\ (-i\tau + \pi)/\sqrt{1-\xi}, & 0 < \xi < 1 \\ -i\theta/\sqrt{\xi-1}, & 1 < \xi. \end{cases} \quad (3.2)$$

The unknown function  $\theta$  can be obtained by applying Cauchy’s integral theorem to  $\chi$  along the real axis of  $\zeta$ , similar to Eq. (2.8). The imaginary part yields

$$\theta(\xi) = \sqrt{\xi-1} \int_0^1 \frac{ds}{\sqrt{1-s}(s-\xi)}, \quad (3.3)$$

and integrating we obtain

$$\theta(\xi) = -2 \arctan \left( \frac{1}{\sqrt{\xi-1}} \right) \quad (3.4)$$

for  $\xi > 1$ . (We may check that  $\theta \rightarrow -\pi$  as  $\xi \rightarrow 1$ , and  $\theta \rightarrow 0$  as  $\xi \rightarrow \infty$ .) This result is then used to determine the free surface profile, by integrating the real and imaginary parts of Eq. (2.10)

$$\frac{dx}{d\xi} = \frac{\cos \theta}{\pi \xi}, \quad \frac{d\eta}{d\xi} = \frac{\sin \theta}{\pi \xi} \quad (3.5)$$

for  $\tau = 0$ . The contraction coefficient  $\alpha = 1/\eta(1)$  is then obtained, by evaluating

$$\eta(1) = 1 + \frac{1}{\pi} \int_1^\infty \frac{\sin \theta}{s} ds. \quad (3.6)$$

The integral in Eq. (3.6) can be evaluated numerically by the trapezoidal rule, which for infinite Froude number gives  $\alpha = 0.5$  to 4 decimal accuracy using 500 points, in agreement with the result previously given in Ref. [1].

#### 4. Numerical Solution Under Gravity

The nonlinear integral equation (2.6) converts to a set of  $N$  algebraic equations in  $N$  unknowns, if we approximate the integral in Eq. (2.9) by summation in a suitable manner. The interval of integration  $(1, \infty)$  is first truncated to  $(1, T)$ , and then divided into  $N$  subintervals with end points  $1 = \xi_0 < \xi_1 < \dots < \xi_N = T$ , in order to evaluate the  $N$  unknowns  $\theta_j \approx \theta(\xi_j)$  for  $j = 1, 2, \dots, N$ . We choose the truncation value  $T$  to be relatively large, to sufficiently extend the free surface into the far uniform flow region.

In obtaining the  $N$  algebraic equations, we use  $N$  collocation points  $\xi_j^*$  at the mid-point in each subinterval  $(\xi_{j-1}, \xi_j)$ , and determine the corresponding values  $\theta_j^*$  linearly between

$\theta_{j-1}$  and  $\theta_j$ . For each point  $\xi_j^*$ , we have one algebraic equation from the integral equation (2.6), so there are  $N$  equations in the unknowns  $\theta_1, \theta_2, \dots, \theta_N$ . The Froude number  $F$  is a given parameter; and we also have  $\theta_0 = -\pi$  at the edge of the horizontal wall, since we assume that the stream separates from the wall smoothly there.

In order to evaluate the Cauchy principle value for the singular integral in Eq. (2.9), we approximate  $\theta(\xi)$  as a linear variable to evaluate the integral on each interval  $(\xi_{j-1}, \xi_j)$ , such that  $\forall \xi_j^*$  we have  $\tau(\xi_j^*) = \tau_j^*$  where

$$\begin{aligned} \tau_j^* \approx & \log \left| \frac{\xi_j^*}{1 - \xi_j^*} \right| + \frac{1}{\pi} \sum_{l=1}^N (\theta_{l-1} - \theta_l) \\ & + \left\{ \theta_l - (\theta_{l-1} - \theta_l) \left( \frac{\xi_j^* - \xi_l}{\xi_{l-1} - \xi_l} \right) \right\} \log \left| \frac{\xi_l - \xi_j^*}{\xi_{l-1} - \xi_j^*} \right|. \end{aligned} \quad (4.1)$$

Similarly, the integral in Eq. (2.11) determining the free surface coordinate  $\eta(\xi_j^*) = \eta_j^*$  can be evaluated numerically via the trapezoidal rule:

$$\eta_j^* \approx \begin{cases} 1 + \frac{1}{\pi} \frac{e^{-\tau_j^*} \sin \theta_j^*}{\xi_j^*} (\xi_j - \xi_j^*), & j = N \\ \eta_{j+1}^* + \frac{1}{2\pi} \left( \frac{e^{-\tau_j^*} \sin \theta_j^*}{\xi_j^*} + \frac{e^{-\tau_{j+1}^*} \sin \theta_{j+1}^*}{\xi_{j+1}^*} \right) (\xi_{j+1}^* - \xi_j^*), & \text{otherwise.} \end{cases} \quad (4.2)$$

To obtain the contraction coefficient, we need the value  $\eta(\xi_0)$ , approximated by

$$\eta(\xi_0) \approx \eta_1^* + \frac{1}{\pi} \frac{e^{-\tau_1^*} \sin \theta_1^*}{\xi_1^*} (\xi_1^* - \xi_0).$$

The closed form may be solved numerically by Newton method provided the iteration converges, and the abscissa  $x_j^* = x(\xi_j^*)$  of the free surface is determined from the real part of Eq. (2.10), approximated by

$$x_j^* \approx \begin{cases} -\frac{1}{\pi} \frac{e^{-\tau_j^*} \cos \theta_j^*}{\xi_j^*} (\xi_j^* - \xi_{j-1}), & j = 1 \\ x_{j-1}^* - \frac{1}{2\pi} \left( \frac{e^{-\tau_j^*} \cos \theta_j^*}{\xi_j^*} + \frac{e^{-\tau_{j-1}^*} \cos \theta_{j-1}^*}{\xi_{j-1}^*} \right) (\xi_j^* - \xi_{j-1}^*), & \text{otherwise.} \end{cases} \quad (4.3)$$

We integrate the real part of Eq. (2.10) from  $\xi_0$  to  $\xi_j^*$  on choosing  $x(1) = 0$ , and then plot the coordinates  $\{(x_j^*, \eta_j^*), j = 0, 1, \dots, N\}$  to get the surface profile.

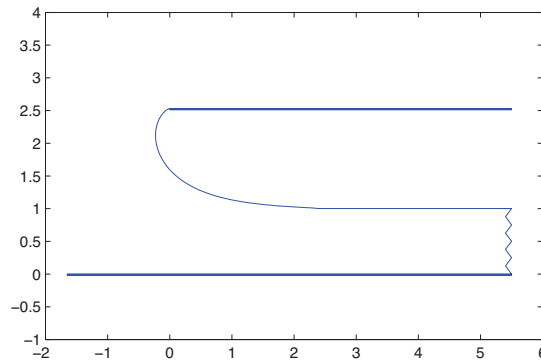


Figure 3: The profile of free surface flow for  $F = 2.1$ , producing contraction coefficient 0.396.

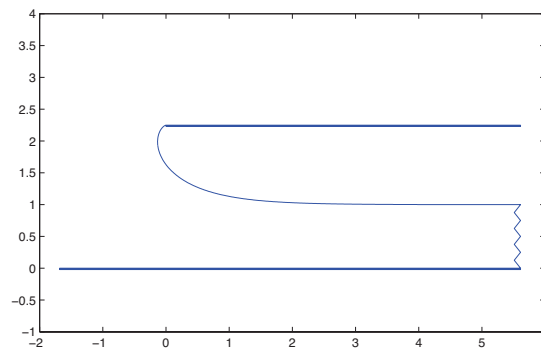


Figure 4: The profile of free surface flow for  $F = 2.5$ , producing contraction coefficient 0.445.

## 5. Results

Most calculations in this paper use  $N = 120$  and  $T \approx 10^7$ , in the numerical procedure described in the previous section. A typical free surface is shown in Fig. 3. The free surface leaves the horizontal wall smoothly; there are no waves on the free surface; and far downstream we see uniform flow with a constant depth smaller than the width of the slit, and their ratio can be calculated for various Froude numbers. For an initial guess of  $\theta$ , we use the result for zero gravity given in Eq. (3.4). For  $\xi > T$ , Eq. (3.4) is  $O(1/\sqrt{\xi})$  such that the improper integral in Eq. (2.9) is convergent, and we can choose large  $T$  so the integral from  $T$  to infinity is negligible.

We computed the free surface using  $F = 2.1$ , plotted in Fig. 3. The profile of the free surface represents the values of  $\theta$  from  $-\pi$  asymptotically to zero, as  $\xi$  ranges from 1 to  $\infty$ . Far downstream the stream tends to uniform flow, and we chose to the uniform depth to be of unit length, such that the contraction coefficient  $\alpha$  is 0.396. For other values of Froude number, our numerical procedure produces a similar free surface, but with lower width  $\eta(1)$  of the slit for larger Froude number. The free surface for  $F = 2.5$  is shown in Fig. 4, with a larger contraction coefficient 0.445. We calculated up to  $F = 15$ , and

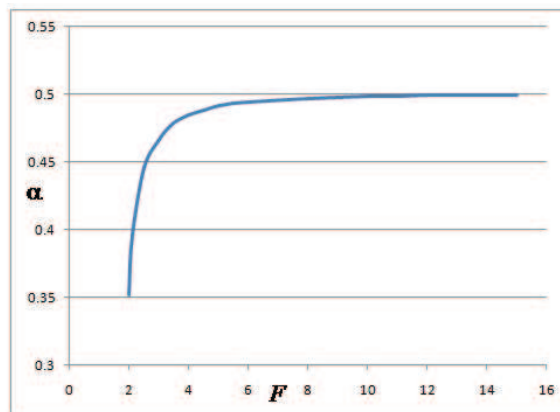


Figure 5: Plot of the contraction coefficient  $\alpha$  versus Froude number  $F$ .

obtained  $\eta(1) = 2.001$  or  $\alpha = 0.499$ . A plot of  $\alpha$  versus  $F$  is given in Fig. 5, where the curve is relatively flat for larger Froude number. Our numerical procedure failed for  $F < 2$ , as indicated by the oscillatory values of  $\theta$  for large  $\xi$  and that the uniform flow far downstream is not met.

For  $F \rightarrow \infty$ , our integral equation is Eq. (2.9) on substituting  $\tau = 0$ , instead of Eq. (2.6). We determined the  $\theta_j$  that satisfy the discrete equation (4.1) for  $\tau_j^* = 0$ . The system of equations was constructed for each  $\xi_j^*$ , and solved by Newton's method. In the post-processing, the coordinates of the free surface were then evaluated from Eq. (3.5). The number  $N$  of the discrete points plays an important role in monitoring the accuracy of the calculation. The truncation number  $T$  is less significant, as  $\theta$  is very small for  $\xi > T$ . Using  $N = 120$ , our calculation gave up to 3 decimal place accuracy. We calculated the contraction coefficients  $\alpha$  for  $N = 30, 60$  and  $120$ ; and those numbers were used to determine  $\alpha$  at  $N \rightarrow \infty$  by

$$\alpha_N = \alpha_\infty + Q \left( \frac{N_{max}}{N} \right)^\delta.$$

The constants  $\alpha_N$  and  $\alpha_\infty$  are the contraction coefficients at that number of discrete points,  $N_{max}$  was chosen to be 120, and  $Q$  and  $\delta$  are constants we determined from our calculations. We obtained  $\alpha_{30} = 0.4879134$ ,  $\alpha_{60} = 0.4982664$  and  $\alpha_{120} = 0.5002489$ , together with  $\beta = 2.4$  and  $Q = -3.0 \cdot 10^{-4}$ , so that by using  $N = 120$  our calculation  $\alpha_{120}$  is accurate up to 3 decimals compared to  $\alpha_\infty = 0.49997$ . This contraction coefficient is the asymptotic number of the curve in Fig. 4, and agrees with the analytical solution presented by Milne-Thomson [1].

## 6. Conclusion

We have discussed a two-dimensional approximation to the flow into the upper part of Borda's mouthpiece, in analysis also applicable to flow under a sluice gate. The free surface flow is described by formulating the problem as an integral equation and using a

boundary element method. The contraction coefficient is found to be less than the known zero gravity value of  $1/2$ , but tends to this value as the Froude number tends to infinity.

### Acknowledgments

The research of this paper was supported by research grants from Bandung Institute of Technology, under contract no. 408/l.1.c01/PL/2012 and 413/l.1.c01/PL/2012.

### References

- [1] L. M. MILNE-THOMSON, *Theoretical Hydrodynamics*, Dover Publication, 1996, pp. 307-309.
- [2] L. H. WIRYANTO, J. WIJAYA AND H. B. SUPRIYANTO, *Free surface flow under a sluice gate from deep water*, Bull. Malay. Math. Sci. Soc., 34 (2011), pp. 601-609.
- [3] L. H. WIRYANTO, *A jet emerging from a slit at the corner of quarter plane*, J. KSIAM, 13(4) (2009), pp. 237-245.
- [4] D. D. FRANGMEIER AND T. S. STRELKOFF, *Solution for gravity flow under a sluice gate*, ASCE J. Engng. Mech. Div., 94 (1968), pp. 153-176.
- [5] B. E. LOROCK, *Gravity-affected flow from planer sluice gate*, ASCE J. Engng. Mech. Div., 96 (1969), pp. 1211-1226.
- [6] Y. K. CHUNG, *Solution of flow under sluice gates*, ASCE J. Engng. Mech. Div., 98 (1972), pp. 121-140.
- [7] J. ASAVANANT AND J.-M. VANDEN-BROECK, *Nonlinear free surface flows emerging from vessels and flows under a sluice gate*, J. Austral. Math. Soc., 38 (1996), pp. 63-86.
- [8] J.-M. VANDEN-BROECK, *Numerical calculations of the free-surface flow under a sluice gate*, J. Fluid Mech. 330 (1996), pp. 339-347.
- [9] B. J. BINDER AND J.-M. VANDEN-BROECK, *Free surface flows past surfboards and sluice gates*, Eur. J. Appl. Maths., 16 (2005), pp. 601-619.
- [10] B. J. BINDER AND J.-M. VANDEN-BROECK, *The effect of disturbances on the flows under a sluice gate and past an inclined plate*, J. Fluid Mech., 576 (2007), pp. 475-490.
- [11] J.-M. VANDEN-BROECK AND E. O. TUCK, *Flow near the interaction of a free surface with a vertical wall*, SIAM J. Appl. Math., 54 (1994), pp. 1-33.
- [12] G. DAGAN AND M. P. TULIN, *Two-dimensional free-surface gravity flow past blunt bodies*, J. Fluid Mech., 51 (1972), pp. 529-543.
- [13] S. W. MC CUE AND L. K. FORBES, *Free-surface flows emerging from beneath a semi-infinite plate with constant vorticity*, J. Fluid Mech., 461 (2002), pp. 387-407.
- [14] L. H. WIRYANTO, *Free surface flow under a sluice gate of an inclined wall from deep water*, AMZIAM J. (CTAC 2010), 52 (2011), pp. C792-C805.
- [15] L. H. WIRYANTO AND E. O. TUCK, *A back-turning jet formed by a uniform shallow stream hitting a vertical wall*, in *Differential Equations: Theory, Numerics and Applications*, E. van Groesen and E. Soewono (Eds.), Kluwer Academic Press, Netherlands, 1997, pp. 371-380.
- [16] L. H. WIRYANTO AND E. O. TUCK, *An open-channel flow meeting a barrier and forming one or two jets*, J. Austral. Math. Soc. Vol. 41 (2000), pp. 458-472.
- [17] L. H. WIRYANTO, *Small Froude number solutions of flow caused by a line source*, J. Indones. Math. Soc., 6 (2000), pp. 1-6.
- [18] G. C. HOCKING AND L. K. FORBES, *A note on the flow induced by a line sink beneath a free surface*, J. Austral. Math. Soc. B, 32 (1991), pp. 251-260.

- [19] G. C. HOCKING AND L. K. FORBES, *Subcritical free-surface flow caused by a line source in a fluid of finite depth*, J. Eng. Math., 26 (1992), pp. 455-466.
- [20] L. H. WIRYANTO, *Zero gravity of a jet emerging from a slit*, J. Indones. Math. Soc., 12 (2006), pp. 89-98.